Available online at www.sciencedirect.com
ScienceDirect
Journal of Crystal Growth 303 (2007) 69–73
JOURNAL OF CRYSTAL GROWTH
www.elsevier.com/locate/jcrysgro

Influence of external flows on pattern growth

Dmitry Medvedev[a,b], Thomas Fischaleck[a], Klaus Kassner[a,*]

[a]*Institut für Theoretische Physik, Otto-von-Guericke-Universität Magdeburg, Germany*
[b]*Institute of Hydrodynamics of the Russian Academy of Sciences, Novosibirsk, Russia*

Available online 19 December 2006

Abstract

Non-facetted crystal growth from an undercooled melt in the presence of an external flow is simulated using a phase-field lattice-Boltzmann scheme. The selection parameter σ as a function of the Péclet number *Pe* is found to fall approximately on a single curve for dendritic and doublonic growth patterns, respectively. This has interesting implications for the availability of current selection theories as predictors of growth characteristics under flow. The morphology diagram in the plane undercooling versus anisotropy is studied as a function of the imposed flow. We find that when the flow speed is increased, the transition line from dendrites to doublons moves so as to favour dendritic patterns, becoming faster than doublons. Moreover, the growth of a single finger in a narrow channel is studied. With increasing flow velocity, the finger width at steady state becomes larger. Our results suggest that stationary growth is impossible in sufficiently fast flows.

PACS: 47.54.−r; 47.20.Hw; 02.70.−c; 68.70.+w

Keywords: A1. Computer simulation; A1. Convection; A1. Dendrites; A2. Growth from melt

1. Introduction

Crystal growth from the melt almost never occurs in convection-free conditions. Nevertheless, models of solidification in the past often focused, when dealing with morphological stability and pattern formation, on situations where convection is absent, because it was difficult to include, while the basic prototypes of patterns appear and may be studied without convection. After the advent of efficient phase-field techniques [1], simplifying the solution of the moving-boundary problem, first simulations of convection in dendritic growth were performed, with both imposed flows and natural convection [2,3]. It was then a natural idea to supplement the efficient approach to interface motion by an efficient non-iterative method for flow simulation, the lattice-Boltzmann scheme [4–8], which is the route taken here.

At present, there is a well-developed theory essentially for purely diffusion-limited dendritic growth, both in two and three dimensions [9–14]. One of its more surprising predictions was the nonexistence of dendrites in the absence of any kind of anisotropy. Due to the nature of the theoretical approach, singular perturbation theory about an Ivantsov solution [15], such a statement can hold only for needle crystals with a shape close to the (exact) solution of which they are supposed to be small perturbations. Indeed, it turned out later that steady-state crystal growth at zero anisotropy *is* possible, but only with a shape that is far from an Ivantsov parabola. These new structures were called doublons [16,17]. Since they continue to exist at finite anisotropy, there is a coexistence range with dendrites, which means that there are two attractors of the dynamics. The standard argument is then that the faster of the two morphologies will win. Large scale two-dimensional structures consist of arrays of dendrites or doublons evolving in a noisy environment via side branching or tip splitting processes. Based on scaling arguments and selection theory, a kinetic phase diagram in

*Corresponding author. Tel.: +49 391 67 18799; fax: +49 391 67 11205.
E-mail address: Klaus.Kassner@physik.uni-magdeburg.de (K. Kassner).

0022-0248/$ - see front matter © 2006 Published by Elsevier B.V.
doi:10.1016/j.jcrysgro.2006.10.227

the parameter space of undercooling versus surface tension anisotropy can be inferred [18].

A first attempt to extend selection theory to situations with a flow was made by Bouissou and Pelcé [19]. This theory is based on a linearization of the basic equations, an approach that has not always been found to be reliable [20]. Clearly, to check the existing theories and guide further theoretical development more numerical or experimental data are needed, some of which the current article will hopefully contribute.

In Section 2, we give the basic model equations and describe their numerical implementation. Section 3 studies the influence of a parallel flow on the selection parameter, whereas in Section 4 changes of the morphology diagram induced by the flow are discussed. Section 5 is devoted to growth in narrow channels, Section 6 to the conclusions.

2. Model

For simplicity, we consider the symmetric model with equal thermal diffusivities of the solid and liquid phases, in two dimensions. The description then starts from the following set of bulk and interface equations:

$$\partial_t u + \mathbf{U}\nabla u = D\nabla^2 u,$$

$$\mathbf{n}\cdot\mathbf{V} = D\mathbf{n}\cdot(\nabla u|_s - \nabla u|_l), \quad u_i = -d(\theta)\kappa. \tag{1}$$

Here, $\mathbf{U}$ is the flow velocity, whereas $u = c_p(T - T_m)/L$ with c_p denoting the heat capacity and L the latent heat, both per unit volume, is a nondimensionalized temperature, T being the local temperature and T_m the bulk melting temperature. D is the thermal diffusivity, $\mathbf{n}$ the normal to the liquid–solid interface, and $\mathbf{V}$ the interface velocity. The subscripts of the field gradients in the second equation refer to the solid and the liquid sides of the interface. $d(\theta)$ is the capillary length, θ the angle between the interface normal and some fixed direction, and κ the interface curvature. At infinity, the temperature in the solid approaches T_m, i.e. $u \to 0$, whereas in the liquid, it takes on some value $T_\infty < T_m$, i.e. $u \to -\Delta$. $\Delta = c_p(T_m - T_\infty)/L$ is the nondimensional undercooling.

We assume the melt to be an incompressible Newtonian fluid, governed by the Navier–Stokes equations, supplemented with boundary conditions at the interface

$$\partial_t \mathbf{U} + \mathbf{U}\nabla\mathbf{U} = -\frac{\nabla P}{\rho} + \nu\nabla^2\mathbf{U}, \quad \nabla\cdot\mathbf{U} = 0, \quad \mathbf{U}_i = 0, \tag{2}$$

where equal mass densities ρ have been assumed in the two phases, ν is the kinematic viscosity, and P denotes the pressure of the liquid. $\mathbf{U}_i$ is the flow velocity at the interface. The boundary conditions correspond to no-slip conditions for the tangential velocity and describe stagnancy of the normal motion in the rest frame of the solid due to the equal densities of the two phases.

It is convenient to use dimensionless variables in the analysis of the growth process. The tip radius can be nondimensionalized using the capillary length as $\bar{R} = R/d_0$, where $d_0 = \gamma_0 T_m c_p/L^2$ is the average of the capillary length over all orientations, γ_0 being the similarly averaged surface tension. Flow and growth velocities become nondimensional via normalization with the characteristic velocity given by the ratio of the thermal diffusion coefficient and the average capillary length, that is $\bar{U} = Ud_0/D$ and $\bar{V} = Vd_0/D$. Properties of the material are characterized by the anisotropy of the capillary length and by the Prandtl number $Pr = \nu/D$, those of the flow by the Reynolds number $Re = UR/\nu$. The capillary length anisotropy is modeled by the usual expression exhibiting four-fold symmetry: $d = d_0(1 - \alpha\cos 4\theta)$.

We use a combined phase-field/lattice-Boltzmann scheme where solidification is simulated with the phase-field model of Karma and Rappel [21,22], and the flow of the liquid as well as convective and diffusive heat transport are modelled with a lattice-Boltzmann method. This means that the actual equations simulated are not those given above but a phase-field approximation to the interface dynamics and a set of kinetic equations that are asymptotically equivalent to the Navier–Stokes and advection–diffusion equations. A detailed description of the scheme is given in Refs. [7,8,23].

3. Growth parameter selection

The growth of a single needle crystal in parallel flow was simulated for fixed surface tension anisotropy and a range of undercoolings and flow velocities. Details of the numerical procedure, the system and grid sizes and convergence considerations may be found in Ref. [23]. Computed values of the selection parameter $\sigma = 2Dd_0/R^2V = 2/\bar{R}^2\bar{V}$ are plotted versus the growth Péclet number $Pe = RV/2D = \bar{R}\bar{V}/2$ in Fig. 1 for dendrites (single symmetric fingers) as well as for doublons (asymmetric fingers). In the figure, $\alpha = 0.75$ for dendrites and $\alpha = 0.3$ for doublons, Δ extends from 0.4 to 0.8, and the reduced flow velocity $\bar{U}$ is typically chosen between 0 and 0.32 (0, 0.01, 0.02, 0.04, etc.). For each of the two data sets most of the points fall onto a unique curve with minor deviations for small Prandtl numbers and large flow velocities.

In the absence of flow, the growth Péclet number depends only on the undercooling. As soon as the flow is introduced, it depends both on the undercooling and the velocity of the imposed flow. What Fig. 1 then tells us is that no matter how we produce a given Péclet number, we should expect the same selected value of σ at fixed anisotropy. Hence, the case with flow can be mapped to the case without flow, i.e., the theory of dendritic growth without convection can be used to make predictions of selected velocities and tip radii in the presence of a forced flow. Of course, the problem of determining the Péclet number, for given undercooling and flow velocity at infinity, is in itself a nontrivial task. In limiting cases (small external flow speed), it may be approximated by the

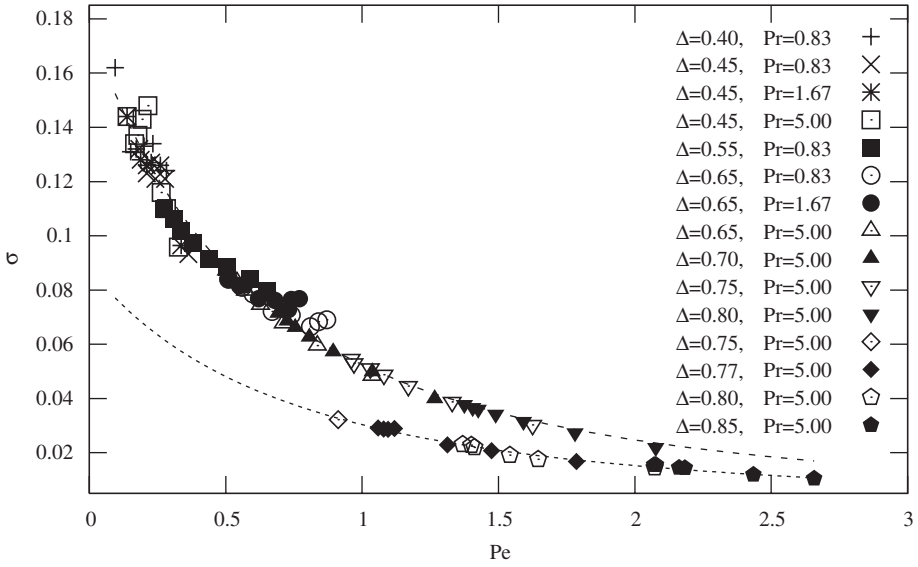

Fig. 1. Dependence of the selection parameter σ on the Péclet number for dendrites (upper curve) and doublons (lower curve). Each symbol corresponds to several flow velocity values at fixed Δ and Pr. The dashed lines are fits explained in the text.

value obtained for an Ivantsov-type solution of an Oseen approximation to the problem with flow.

According to selection theory for the purely diffusion-limited case, we should expect σ to become independent of the Péclet number for small anisotropy and small undercooling. The latter condition can be relaxed [24]—as long as $Pe\alpha^{1/2} \ll 1$, the standard result $V \sim (D/d_0)\alpha^{7/4}Pe^2$ continues to hold for our fourfold model anisotropy. However, computational limitations render this limit difficult to access, hence neither of these conditions is well satisfied in Fig. 1, where $\alpha = 0.75$ or 0.3 and Pe varies through 1. The opposite limit of large Péclet number is also known analytically [24]; the selection parameter should vary, for fixed small anisotropy, proportional to $1/Pe^2$. Moreover, it is possible to evaluate the predictions of solvability theory [25] numerically for arbitrary Péclet numbers, which gives a curve of very similar appearance to the top curve in Fig. 1 [23].

Because the theory predicts the limiting behaviours of the selection parameter at small and large Péclet numbers, it is tempting to try to capture the behaviour at intermediate Pe by a simple interpolating function. The simplest rational function approaching a constant value for $Pe \to 0$ at finite slope and being proportional to $1/Pe^2$ at large Pe is $f(Pe) = a/(1 + bPe)^2$. Fits with this function work pretty well for both our numerical data (as is demonstrated in Fig. 1) and the results from selection theory [23], surprisingly also for the case of doublons.

4. Morphology diagram

The kinetic phase diagram derived for purely diffusive growth [18] distinguishes four morphologies: compact dendritic structures at large anisotropy and not too large undercooling, compact seaweed patterns at large undercooling, and noise-dominated fractal dendritic and seaweed morphologies at sufficiently small anisotropy and undercooling, respectively. The transition lines between the different morphologies and their nature (as first- or second-order kinetic phase transition or cross-over) were determined analytically under certain limit assumptions [18]. Doublons were found to cease to exist at larger anisotropies, but when they exist, they are faster than dendrites. In principle, the latter exist at all nonzero anisotropies, but they are overtaken and thus overgrown by doublons in the region of coexistence. How external flow may influence the different growth patterns is interesting and largely unexplored.

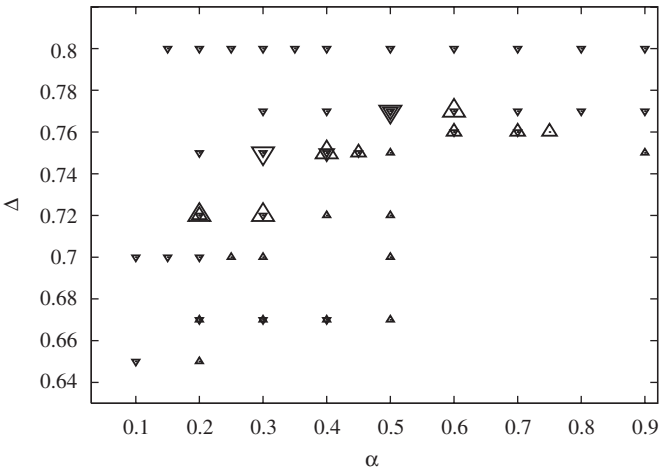

Fig. 2. Morphology diagram displaying the predominance of dendrites or doublons at different flow speeds.

In the present work, we study the morphology diagram for growth in a parallel counterflow, imposing a number of different flow velocities, with a view to the positions of the

transition lines between doublon and dendrite growth. Fig. 2 gives an overview of the measured morphology diagram (a small section only of the plane undercooling versus anisotropy) for the diffusive case and two different flow velocities. Our results for zero flow agree well with simulations by Tokunaga and Sakaguchi [26].

The case of purely diffusive growth is depicted in Fig. 2 by the smallest symbols. Triangles with their tips pointing upwards correspond to dendrites, inverted triangles to doublons. On increase of the reduced flow velocity $\bar{U}$ to 0.01, denoted by larger triangles, dendrites become faster than doublons at several combinations of undercooling and anisotropy. The largest triangles in Fig. 2 correspond to a velocity of $\bar{U} = 0.04$. They demonstrate how the region where dendrites are faster than doublons increases with increasing flow velocity.

Note that the morphology diagram should actually be displayed in three dimensions, as it is spanned by the three variables α, Δ, and $\bar{U}$. We circumvent the need for a genuine three-dimensional representation by taking different symbol sizes to represent different flows, as only few flow-velocity values could be studied so far.

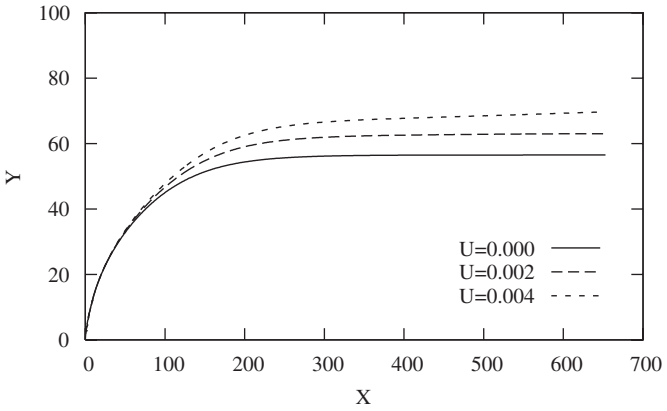

Fig. 3. Steady-state finger shapes for $\Delta = 0.55$ and flow velocities $\bar{U} = 0$, 0.002, and 0.004. Note the difference in scale for X and Y.

Table 1

U	0	0.0005	0.001	0.002	0.004
x_{calc}	0.55	0.567	0.583	0.615	0.676
x_{meas}	0.55	0.567	0.583	0.615	0.683

5. Channel growth

When a two-dimensional needle crystal grows in free space and side branching is suppressed (which is easier to do numerically than in experiment), it will ultimately assume a parabolic shape. In reality, growth is normally confined by container walls or other dendrites. Then the overall shape changes, often taking the general appearance of a Saffman–Taylor finger. Channel growth may have a certain relevance in assessing the question of the dynamics of whole arrays of dendrites or doublons. Therefore, it is interesting to study the influence of flow in such a geometry as well. We restrict ourselves to some preliminary considerations here and hope to report on a more extensive investigation in the future.

It is easy to see that even the simple basic state of a constant-width finger moving at constant velocity must change in a parallel counterflow. In the diffusion-limited case, energy conservation requires its width to be—assuming equal densities of the liquid and the solid—equal to the product of the channel width and the undercooling. If we wish to generalize this to the case of different densities, we must consider mass conservation as well and admit that a flow is generated behind the tip of the advancing finger even if there was none to begin with. Establishing the mass and energy balances between the regions far ahead and far behind the tip, we get $x = (1 + U/V)\Delta/n$ for the relative width x of the growing finger. $n = \rho_s/\rho_l$ is the ratio of solid and liquid mass densities.

For $U \neq 0$, the finger width appears to increase with increasing flow velocity. Because the expression for x includes the unknown growth velocity V, all we can say with certainty from the formula is that the finger width becomes larger in comparison with the flowless case (because $U/V > 0$). A detailed discussion of the behaviour beyond small flow velocities requires knowledge of V, which changes with U for given Δ. Nevertheless, the formula at least suggests that with increasing flow velocity the finger width will also increase; moreover, it implies an upper bound for U/V, hence a critical flow velocity might exist, beyond which stationary growth becomes impossible (the velocity for which $x = 1$). The only way to avoid this would be to have V increase proportionally to U or faster at large U.

That the finger width increases with increasing flow velocity is confirmed by simulations. The shapes of a few numerically grown fingers are shown in Fig. 3, measured and calculated values of x (with V taken from the simulation) in Table 1.

There is good agreement between theory and simulation data. Moreover, simulations indicate also that indeed no steady state is attained for large flow velocities. This behaviour is probably related to the prediction by Bouissou and Pelcé for free growth that beyond a critical flow speed steady-state solutions become impossible [19].

6. Conclusions

To sum up, we have simulated dendritic growth from a supercooled melt in external counterflows antiparallel to the needle crystal, using a combined phase-field/lattice-Boltzmann scheme. Several regions of the morphology diagram in the space spanned by the anisotropy parameter, the nondimensional undercooling and the nondimensional flow velocity have been explored.

For dendrites at moderate to high undercooling and high anisotropy, we find that the values of tip radius and selection parameter, and hence of the growth velocity, depend on the growth Péclet number only, not on the undercooling and flow velocity separately. Hence, it may be argued that the essential effect of a parallel flow, at least in a certain part of the parameter space, is to change the selected tip radius and growth velocity solely by modifying (increasing) the Péclet number. In this region, selection theory for the purely diffusive case is applicable, the main task being to determine the relationship between undercooling, imposed flow velocity and the growth Péclet number. With doublons, a similar dependence is obtained for the selection characteristics.

For smaller anisotropy, an interesting phenomenon is observed. The growth velocity for dendrites increases faster than for doublons with increase of the flow velocity (at the same undercooling and anisotropy). For some parameters, dendrites become faster, hence, external flow can lead to morphology transitions and change the kinetic phase diagram.

Acknowledgements

Financial support of this work by the German Research Foundation (DFG) under Grant no. FOR 301/2-1 is gratefully acknowledged.

References

[1] A. Karma, W.-J. Rappel, Phys. Rev. Lett. 77 (1996) 4050.
[2] R. Tönhardt, G. Amberg, J. Crystal Growth 194 (1998) 406.
[3] C. Beckermann, H.-J. Diepers, I. Steinbach, A. Karma, X. Tong, J. Comput. Phys. 154 (1999) 468.
[4] W. Miller, S. Succi, D. Mansutti, Phys. Rev. Lett. 86 (2001) 3578.
[5] W. Miller, S. Succi, J. Stat. Phys. 107 (2002) 173.
[6] W. Miller, Int. J. Mod. Phys. B 17 (2003) 227.
[7] D. Medvedev, K. Kassner, J. Crystal Growth 275 (2005) e1495.
[8] D. Medvedev, K. Kassner, Phys. Rev. E 72 (2005) 056703.
[9] B. Caroli, C. Caroli, B. Roulet, J. Langer, Phys. Rev. A 33 (1986) 442.
[10] M. Ben Amar, Y. Pomeau, Europhys. Lett. 2 (1986) 307.
[11] A. Barbieri, D. Hong, J. Langer, Phys. Rev. A 35 (1987) 1802.
[12] S. Tanveer, Phys. Rev. A 40 (1989) 4756.
[13] M. Ben-Amar, E. Brener, Phys. Rev. Lett. 71 (1993) 589.
[14] E. Brener, Phys. Rev. Lett. 71 (1993) 3653.
[15] G.P. Ivantsov, Dokl. Akad. Naut. SSSR 58 (1947) 567.
[16] T. Ihle, H. Müller-Krumbhaar, Phys. Rev. E 49 (1994) 2972.
[17] M. Ben-Amar, E. Brener, Phys. Rev. Lett. 75 (1995) 561.
[18] E. Brener, H. Müller-Krumbhaar, D. Temkin, Phys. Rev. E 54 (1996) 2714.
[19] P. Bouissou, P. Pelcé, Phys. Rev. A 40 (1989) 6673.
[20] S. Tanveer, J. Fluid Mech. 409 (2000) 273.
[21] A. Karma, W.-J. Rappel, Phys. Rev. E 53 (1996) R3017.
[22] A. Karma, W.-J. Rappel, Phys. Rev. E 57 (1998) 4323.
[23] D. Medvedev, T. Fischaleck, K. Kassner, Phys. Rev. E 74 (2006) 031606.
[24] E. Brener, V. Mel'nikov, Adv. Phys. 40 (1991) 53.
[25] A. Barbieri, J. Langer, Phys. Rev. A 39 (1989) 5314.
[26] S. Tokunaga, H. Sakaguchi, Phys. Rev. E 70 (2004) 011607.